Babeș-Bolyai University
Faculty of Physics

Disordered Graphene Systems and Transition Metal Dichalcogenides. A Theoretical Study on 2D Systems

- Summary -

Teodor-Lucian Biter

Scientific Adviser:
Prof. Dr. Ioan Grosu

Cluj-Napoca
- 2021 -

Abstract

Almost two decades have passed since the discovery of graphene. Following this, two-dimensional systems have received a great deal of attention, resulting in the publishing of a myriad of research papers on them. However, because of their theoretical and technological potential, they still need a great deal of attention. One of the aims of this thesis is to explain certain magnetic measurements done on fluorinated graphene. This is achieved by working in the Born and T-matrix approximations to analyse the static spin susceptibility of gapped graphene systems in the presence of disorder with weak impurity scattering. The results obtained achieved a qualitative agreement with the experimental data. Another model for the study of the static spin susceptibility proposes graphene systems in the presence of disorder with strong impurity scattering (the unitary limit), while considering a small energy gap. This model is proposed as a test for the unitary limit in disordered graphene systems, alongside with our models for the spin-lattice relaxation time and electronic heat capacity, respectively. In all three studies done while working in the unitary limit, we noticed certain behaviour changes that depend on the impurities concentration. Besides graphene, the thermodynamic properties of transition metal dichalcogenide superconductors on a substrate have also been studied. The effects of a substrate on the superconducting energy gap, the specific heat and specific heat jump, and the critical field are analysed.

Keywords: Graphene, Disorder, Energy gap, T-matrix approximation, Born Approximation, Unitary limit, Critical disorder, Spin susceptibility, Spin-lattice relaxation, Electronic heat capacity, Transition metal dichalcogenides, Substrate, Massive gapped spectrum, Superconducting gap, Specific heat, Critical field.

Contents

Abstract **i**

1 Introduction **1**

2 Disordered graphene systems with weak scatterers **4**

2.1 Graphene 4

2.2 Spin susceptibility of disordered graphene systems 6

3 Disordered graphene systems with strong scatterers **10**

3.1 Introduction 10

3.2 Spin susceptibility as a test of unitary limit in disordered graphene systems . . . 10

3.3 Spin-lattice Relaxation Time in Disordered Graphene Systems 13

3.4 Electronic heat capacity in disordered graphene systems 15

4 Transition metal dichalcogenide superconductors **19**

4.1 Introduction 19

4.2 General concepts 20

4.2.1 Superconductivity in transition metal dichalcogenides 21

4.3 Thermodynamic properties of transition metal dichalcogenide superconductors on a substrate 22

5 Conclusions and Outlook **28**

Bibliography **30**

Chapter 1

Introduction

Graphene is the first two-dimensional material to have ever been synthesized and it is a one atom thick layer of carbon atoms arranged in a hexagonal, honeycomb-like, lattice [1]. The unusual properties of graphene are owed to the Dirac-like band structure, its valence and conduction bands meet in six points at the corners of the Brillouin zone [2,3], divided into the non-equivalent points labeled K and K', also named Dirac points [4]. The linear energy dispersion around the Dirac points gives rise to the many interesting physical phenomena present in graphene systems [4, 5]. In spite of its outstanding properties, pristine graphene is not well suited for many practical application due to its zero bandgap. At the same time, one has to consider that fabricated graphene samples are not free of structural defects and that the properties of graphene can be affected by the presence of disorder. The density of states is one of them and it, in turn, affects many other physical properties. Ever since graphene was synthesized, a great many theoretical studies have been published on the problem of disorder in graphene systems with the purpose to explain the results that were obtained experimentally [4–10]. To achieve this, the authors used different approximations, such as: the Born approximation, the self-consistent Born approximation, the T-matrix, the self-consistent T-matrix approximation, and the unitary limit. The gapped energy spectrum was accounted for in order to obtain a better analysis of the anomalous growth of thermoelectric power in graphene [11] (massive gapped spectrum). In order to explain several spectroscopic measurements [12], the phenomenological massless gapped spectrum was introduced [13]. The latter reconciles the gapped nature of the energy spectrum and the massless character of the particles in graphene.

Not too long ago, the magnetic measurements conducted on fluorinated graphene revealed

strong magnetism in these graphene-based structures [14]. Thus, in order to analyse, in a qualitative way, the static spin susceptibility, that was measured in fluorinated graphene, we have considered a gapped graphene system and worked in the Born and T-matrix approximations [15].

By considering the unitary limit (strong impurity scattering), Ostrovsky et.al. [7] managed to obtain results that compared nicely with the experimentally observed linear electron concentration dependence of the conductivity of graphene [16, 17]. By working in the unitary limit, we proposed to use the temperature dependence of the static spin susceptibility to reveal the presence of scattering mechanisms [18].

Nuclear Magnetic Resonance (NMR) is an experimental technique with far reaching applications in both scientific areas and industry. Strong deviations from the NMR parameters in metals were reported in systems formed of graphene monolayers [19,20]. The differences arise from the Fermi contact term in the electron-nuclear spin interaction that differs significantly from the case of standard metals and the presence of an energy gap has important effects as well. Having this in mind, we proposed to study the spin-lattice relaxation time in the case of disordered graphene systems with strong scatterers (unitary limit) [21].

When considering possible technological applications, the thermal properties of the materials should be taken into account. As such, it is of interest to study the thermal properties of graphene (e.g., heat capacity and thermal conductivity) [22, 23]. Although in graphene the heat capacity is dominated by the contribution from the phonons, one shouldn't rule out the importance of the electronic heat capacity. As such, we proposed to study the electronic heat capacity of graphene is the presence of disorder, while working in the unitary limit [24].

The first synthesis of monolayer graphene from bulk graphite was followed by a massive increase in the number of published articles on graphene. This growing interest in graphene and its interesting physical properties gripped the scientific community and reinvigorated the research done on two-dimensional materials. Transition metal dichalcogenides are a class of quasi two-dimensional layers, bonded by weak van der Waals forces, that have a rich history spanning back over 50 years [25] and has benefited from this boom. At low temperatures, these materials

exhibit s-wave superconductivity and the superconductivity states coexist with charge density waves [26]. Other studies have revealed similar properties to those of high-temperature superconductors, such as the lifetime behaviour of the quasi-particles and the linear dependence of the normal state resistivity with temperature. On the other hand, in the region where the charge density waves gap vanishes, Dirac fermions quasi-particles are created. The superconductivity is then given by these particles that form acoustic phonon mediated Cooper-pairs [27, 28]. They resemble to a degree the superconducting properties in graphene [29, 30]. Following the method given in Ref. [28], we proposed to analyse several thermodynamic properties of the superconducting transition metal dichalcogenides grown on a substrate. In the presence of a substrate, an asymmetry in the Hamiltonian occurs. This is liable to lift the degeneracy at the Dirac points and as a consequence, a non-superconducting energy gap E_0 opens in the energy spectrum [20, 31]. Close to the Dirac point, this leads to the massive gapped spectrum and this is the case that we proposed to be studied, instead of the case of massless gapped spectrum [13] used in Ref. [32] to discuss the gap equation, the critical temperature, and the Geilikman-Kresin ratio [33, 34].

Chapter 2

Disordered graphene systems with weak scatterers

In this chapter we will start with a short review on graphenes and then summarise our findings on the static spin susceptibility for disordered graphene systems.

2.1 Graphene

Carbon is a non-metallic tetravalent chemical element that is a key component of life as we know it and the focus of organic chemistry. One of carbons allotrope, with planar sp^2 hybridization, is graphene, a two-dimensional structure disposed in a hexagonal, honeycomb-like, lattice that can be considered as two interlacing triangular lattices as shown in Fig 2.1.1.

Although graphene was first synthesized almost two decades ago by Novoselov et al. [35,36] (in 2010 Andre Geim and Konstantin Novoselov received the Nobel prize for their groundbreaking experimental work regarding graphene), it has been studied ever since due to its remarkable properties, the band structure was first calculated in 1947 [2] using the tight-binding approximation in order to explain the properties of graphite, a material that was being used in the nuclear reactors of those times; graphene still being a purely theoretical structure as theory predicted that one- or two-dimensional crystalline long-range order was not possible [37, 38]. About a decade after Wallace's studies came the Slonczewski-Weiss-McClure (SWM) band-structure model of graphite [39, 40] that described the electronic properties in graphite and was able to successfully describe the experimental data. A problem of this model was the assignment of the electron and hole states in the material, a problem that was solved in 1968 following laser magnetoreflection experiments on pyrolytic graphite [41], that analysed the type

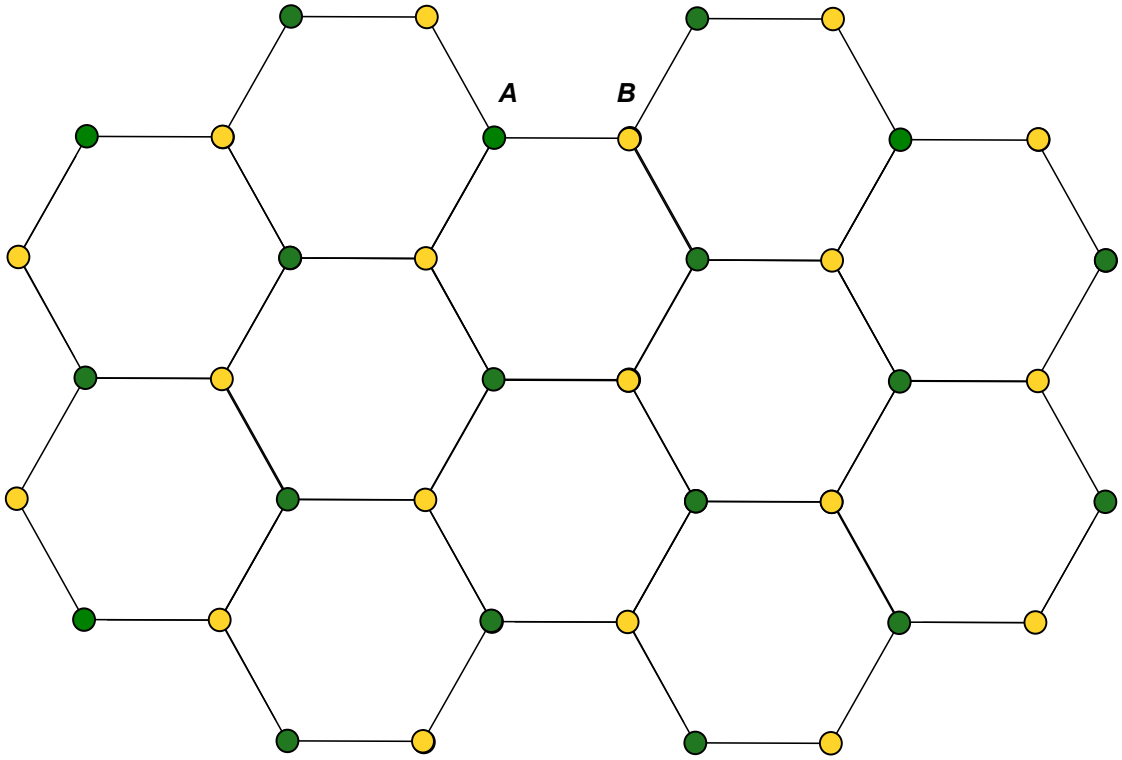

Figure 2.1.1: The graphene honeycomb lattice, A and B are the carbon atoms belonging to the considered triangular lattices.

of carriers at the K points and established their currently accepted location. A major problem of the SWN model was that the band-structure description was unable to describe the van der Waals-like interactions that arise between the graphene layers, but the model was revised in 2003 [42]. Research into this matter is still being conducted [43–45] and although the values obtained by density functional theory are quite scattered, as seen clearly in these comparative studies [46, 47], experimental results are beginning to appear [48, 49]. Even though these problems are lacking in the single-layer graphene crystal, in the multilayer case they are present and of interest as the layered structures can have considerably different electronic properties. Granted that these layered structures are just as interesting, but for this thesis they were only a digression.

The low-energy quasiparticle excitations represents one of the most notable feature of graphene as they are chiral, massless, Dirac fermions that follow a linear dispersion around the Dirac points. This aspect is responsible for many interesting phenomena, as they imitate the massless fermions described by quantum electrodynamic, with the speed of light c being considered to be the Fermi velocity v_F, which is about 300 times smaller. This leads to the presence of quantum

electrodynamic physics in graphene [50]. For the curious reader, more in depth reviews from a theoretical and experimental point of view of graphene can be found in Refs. [4, 51].

2.2 Spin susceptibility of disordered graphene systems

The Green's functions do not work so well when used to describe the scattering of a particle from a single impurity. The changes of a particle's energy is calculated from the interactions by using Dyson's equation, in which the self-energy of a particle contains the energy that stems from the interactions between the particle and environment. In a very large system, a single impurity would induce a change of the particles energy that is inversely proportional to the system's volume V. With the addition of N_i impurities (with $N_i/V = n_i$ as $V \to \text{inf}$), one could change the particles energy. By doing this, the energy of the particle becomes a function of the impurities concentration n_i. To study the isolated impurity case, one has to find the self-energy for n_i and then take the limit $n_i \to 0$ [52].

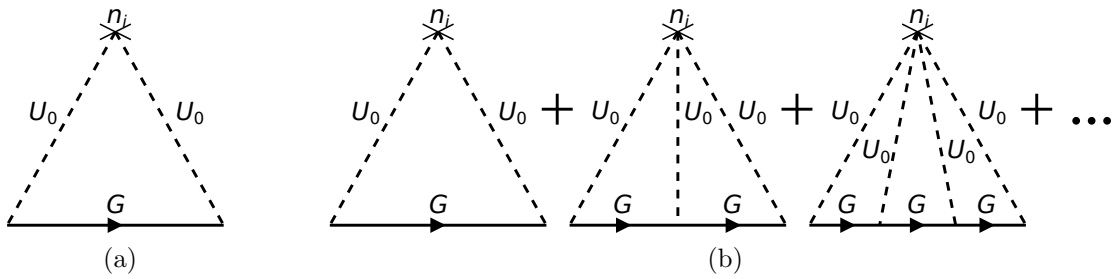

Figure 2.2.1: The Feynman diagram for the (a) Born approximation and (b) T-matrix approximation of the self-energy.

In Fig. 2.2.1 we have the Feynman diagram for the Born approximation and T-matrix approximation of the self-energy. The Born approximation holds true for small impurities concentration and no multiple scattering events. In this case of the T-matrix approximation, one has to consider the summation of the entire series of Feynman diagrams with non-intersecting impurity lines concerning scattering, using the bare Green's function. The density of states was calculated using the self energy. The appropriate density of states that were obtained, were then used to determine the static spin susceptibility for the approximations considered.

In Fig. 2.2.2, we plot the temperature dependence of the spin susceptibility for the Born approximation case using the appropriate density of states and self-energy. We chose to consider

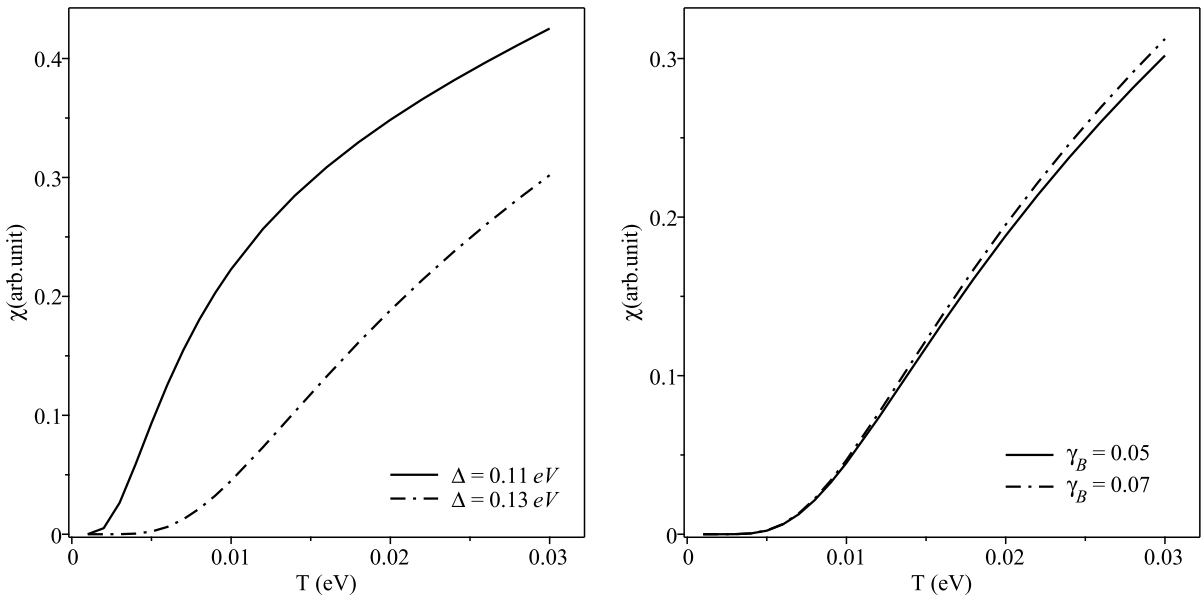

Figure 2.2.2: The spin susceptibility as a function of temperature, in the Born approximation, for (a) $\Delta = 0.11$ eV (line) and $\Delta = 0.13$ eV (dashed-dotted-line), using $\varepsilon_c = 5$ eV, $\mu = 0.1$ eV, $\gamma_B = 0.05$ and (b) $\gamma_B = 0.05$ (line) and $\gamma_B = 0.07$ (dashed-dotted-line), using $\varepsilon_c = 5$ eV, $\mu = 0.1$ eV, $\Delta = 0.13$ eV.

the chemical potential μ as a parameter, but, this is an assumption that doesn't hold true for the entire temperature interval. However, in our case, where the temperatures are lower than 300K, approximating the chemical potential with a constant value is acceptable if we consider the extrinsic graphene case and low disorder (see Refs. [10, 53]). For the clean case and in the extrinsic limit, we found that $\mu(T = 200\text{ K}) \simeq 0.75E_F$, which means that our numerical estimations with a constant value approximation for the chemical potential ($\mu \approx E_F$) are less reliable close to the room temperature. However, the slight decrease of the chemical potential in this temperature range can explain the plateau structure in the temperature dependence of the static spin susceptibility from the experiments [14]. In the presence of disorder, it is very difficult to estimate the chemical potential because of the complicated form of the density of states that we found. This estimation would need a separate investigation, using numerical methods. However, in the limit of low disorder we assumed the above approximation, considering that the effect of the impurities is small. Due to the symmetric form of the density of states, these results do not change if $\mu \to -\mu$ (holes contribution). In Fig. 2.2.2(b) we analyse the effect of weak disorder on the temperature dependence of the spin susceptibility. This effect

is very small as long as we consider the weak disorder case only, where γ_B is small. The weak disorder assumptions means that the impurities concentration is small, thus, the disorder can be considered as Gaussian and $\gamma_B \ll 1$ (see Refs. [7, 9]). For example, if we take the impurity density $n_i \sim 10^{11}$ cm^{-2} and the potential strength $U_0 \sim 1$ KeVÅ^2, the strength of disorderness is evaluated to $\gamma_B \sim 0.1$ [9]. In our estimations we assume an impurity density lower than 10^{11} cm^{-2} and the strengths of order for $\gamma_B = 0.05$ and $\gamma_B = 0.07$ are considered as reliable.

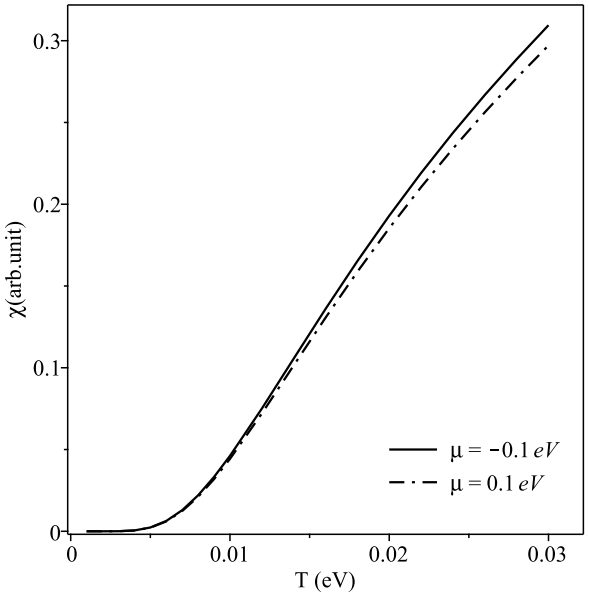

Figure 2.2.3: The spin susceptibility as a function of temperature, in the T-matrix approximation for $\mu = -0.1$ eV (line) and $\mu = 0.1$ eV (dashed-dotted-line), using $\varepsilon_c = 5$ eV, $\gamma_B = 0.05$, $\Delta = 0.13$ eV, $u = 1$ (eV)$^{-1}$.

In the T-matrix approximation case, again, the distance between the energy-gap and the chemical potential is important and the density of states is no longer symmetric (in energy) and the temperature dependence of the spin susceptibility differs for the cases when $\mu > 0$ and $\mu < 0$, as one can see from Fig. 2.2.3. Here, the effect of weak disorder on the temperature dependence of the spin susceptibility was found to be small.

Even simplified, our model still revealed additional information on how different parameters influence the temperature dependence of the static spin susceptibility (the authors in Ref. [14] used only a simple exponential temperature dependence in the presence of a gap). As such, the first important information present in our model is on the effect the position of the chemical potential relative to the gap has on the temperature dependence of the static spin susceptibil-

ity. This effect produces important modifications in the temperature dependence of the spin susceptibility in both the Born and the T-matrix approximations. This was to be expected, as at finite temperatures, the relative position of the chemical potential to the gap strongly influences the number of electrons (holes) in the system. The second information is how the weak disorder influences the temperature dependence of the static spin susceptibility. The effect of weak disorder has in the Born approximation, as well as in the T-matrix approximation, is a small one (with small differences between the approximations, as mentioned). Even though we have achieved a qualitative agreement between theory and experiment, in the next chapter, among other properties, we will summarise our investigations on the static spin susceptibility, while considering the opposite case of weak scatterers.

Chapter 3

Disordered graphene systems with strong scatterers

3.1 Introduction

We've seen in the previous chapter that we have managed to achieve a qualitative agreement between theory and experiment for the static spin susceptibility. In this chapter we will summarise our studies on the static spin susceptibility, the spin-lattice relaxation parameter T_1, and the electronic heat capacity of disordered graphene systems while considering strong impurity scattering (i.e., the unitary limit $U_0 \to \infty$). The study conducted by Ostrovsky et.al. [7] has shown that the unitary limit can be successfully used to describe experimental data, as they managed to obtain results that compared nicely with the experimentally observed linear electron concentration dependence of the conductivity of graphene [16, 17].

3.2 Spin susceptibility as a test of unitary limit in disordered graphene systems

The static spin susceptibility of graphene systems was analysed in the presence of disorder and a small energy gap. We looked into the effects the temperature and impurity concentration have on the static spin susceptibility. We considered the scattering mechanism in the unitary limit to be of main importance and a small energy gap of secondary importance. To achieve our goal, we have first calculated the electron's self-energy while working in the unitary limit and considering a small gap. Those results were then used to calculate the density of states, with the help of which we determined the static spin susceptibility.

In order to find out the electron's self-energy, we considered disorder induced by randomly

distributed impurities. The self-energy Σ in the presence of impurities is given by the complete impurity's T-matrix [7, 9, 54]. Usually, the self-energy represents the contribution to the particle's energy due to the interactions between the particle and the system (here the scattering events). In the presence of impurities, momentum eigenstates are no longer energy eigenstates. The inverse lifetime is the energy uncertainty of a momentum eigenstate and the mean free path is the momentum uncertainty of an energy eigenstate. As a consequence, the electron Green's function, in the real space, decays exponentially (instead of a power law behaviour for a clean system). U_0 corresponds to the Fourier transform of the impurity potential, whose range can be long or short (unscreened or screened). We considered short-range impurities which result from localized structural defects in the honeycomb lattice. These impurities are roughly on the length scale of the lattice constant, when it is acceptable to approximate $U(\vec{k}) = U_0$, a real constant. Point defects can nucleate a few electronic states in their vicinity, which leads to a change in the electronic density and to an enhancement of the density of states at the Dirac Point, in contrast to the clean case where the density of states vanishes.

The chemical potential will vary slightly in the interval of temperatures that goes from $T = 0$ K and up to room temperature, in our case $\mu = E_F$ for $T = 0$ K and $\mu = 0.7E_F$ for $T = 300$ K, where E_F is the Fermi energy. Taking this variation into account, in Fig. 3.2.1 we plot the temperature dependence of the static susceptibility for two different dimensionless concentration of impurities, $\eta < \eta_c$ and $\eta > \eta_c$. Here, η_c is a critical value of the impurities concentration that we determined analytically. The spin susceptibility has finite, non-zero, values at $T = 0$ K due to the fact that in disordered graphene, near the Dirac point, the density of states is enhanced by impurities instead of being suppressed as $|E|$ ($E \to 0$), a result valid for the clean case. In Fig. 3.2.2 we plot the temperature dependence of the spin susceptibility for several values of the dimensionless concentration of impurities. We observe two different behaviours. If the degree of disorder is less than a critical value η_c (for the values used $\eta_c = 0.031$), the temperature dependence of the spin susceptibility starts from a single point, that is mainly determined by the Fermi energy. If the degree of disorder is enhanced ($\eta > \eta_c$), the behaviour at $T = 0$ K is different, being disorder dependent. This behaviour remains valid even for the case when the value of the energy gap tends to zero. This kind of temperature dependence of

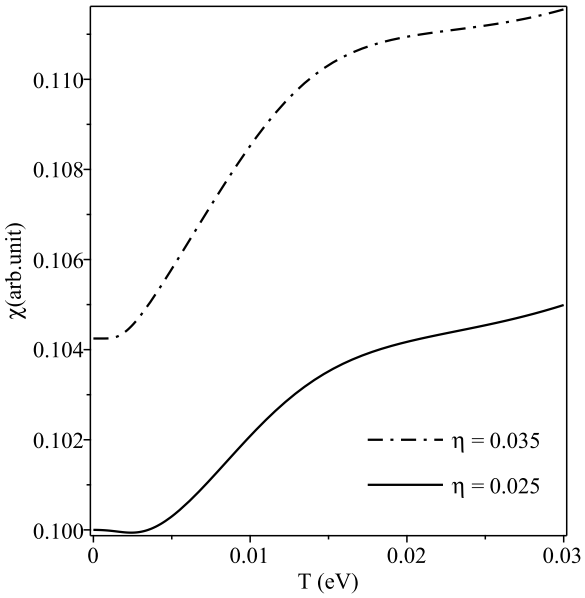

Figure 3.2.1: Static spin susceptibility as function of temperature for: $\eta = 0.035$ $(\eta > \eta_c)$, and $\eta = 0.025$ $(\eta < \eta_c)$, with: $\Delta = 0.05\ eV$; $E_F = 0.1\ eV$; $E_c = 1\ eV$

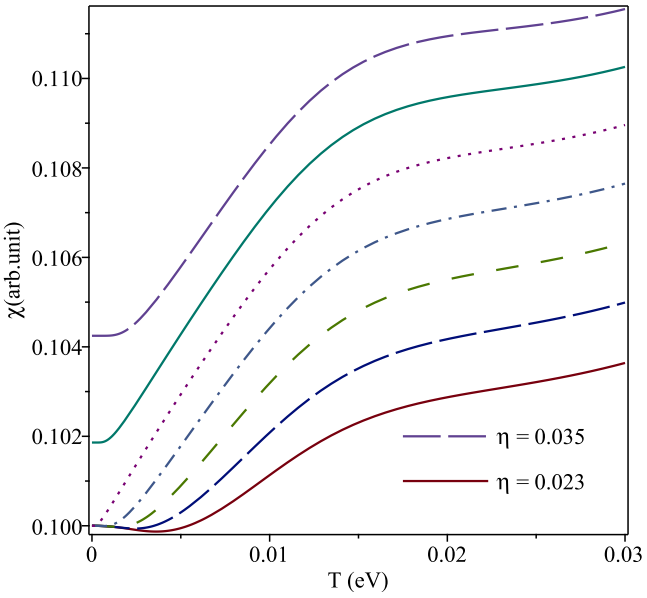

Figure 3.2.2: Static spin susceptibility as function of temperature for several values of η (with an incremented of 0.002). The lower curve corresponds to $\eta = 0.023$, the upper curve to $\eta = 0.035$, and the dotted curve to the critical disorder $\eta_c = 0.031$, with: $\Delta = 0.05\ eV$; $E_F = 0.1\ eV$, $E_c = 1\ eV$.

the static spin susceptibility could be an additional test to the presence of strong scatterers in graphene systems. However, the experimental results from Ref. [14], concerning the temperature dependence of the static spin susceptibility, are rather closer to the Born approximation (weak scatterers, Gaussian disorder) in the presence of an energy gap than to the unitary limit; i.e, the analysis of the experimental results we did in the previous chapter Ref. [15], where we pointed

out the importance of the energy gap rather than the small influence of disorder. However, in Ref. [14] the presence of disorder is presumed to be accidental rather than engineered by the authors. The model we developed here captures the important (almost linear) increase of the spin susceptibility with temperature, which is a signature of the presence of Dirac fermions through the appropriate density of states (see Ref. [6]).

If the unitary limit is indeed important, one could observe this behaviour in future experimental measurements by carefully engineering the presence of disorder in graphene systems. The plot of the magnetic susceptibility as a function of T reveals the presence of the Dirac fermions through the linear part of the plot and that the graphenes static spin susceptibility increases with both temperature and number of impurities. This seems to be a general result which appears even for finite U_0 [6].

3.3 Spin-lattice Relaxation Time in Disordered Graphene Systems

Nuclear Magnetic Resonance (NMR) is an important experimental technique for the scientific and industrial areas. The phenomenon occurs when on the polarized nuclei of the sample, by a strong magnetic field, is applied another weak perpendicular oscillating magnetic field at the resonant frequency that induces an energy transition in the nuclear system. Then the nuclear magnetic relaxation is studied and, usually, it is caused by magnetic and quadrupole interactions between a nuclear magnetic moment and the surrounding electrons [55, 56]. The spin-lattice relaxation process, when the nuclei interact with the lattice to return to a lower energy level, is characterised by the spin-lattice relaxation time (in an usual metal $1/(T_1T) \sim const$). In graphenes, it has been reported that the NMR parameters have strong deviations from those in metals [19,20]. The difference of the Fermi contact term in the electron-nuclear spin interaction between standard metals and graphene is the reason these differences arise; the presence of an energy gap was reported to have important effects as well. The NMR parameters for three-dimensional Dirac electron systems in the presence of the orbital and quadrupole interactions have also been studied [57]. Here we will summarise our analysis of the spin-lattice relaxation time of graphene systems in the presence of disorder with strong impurity scattering (unitary

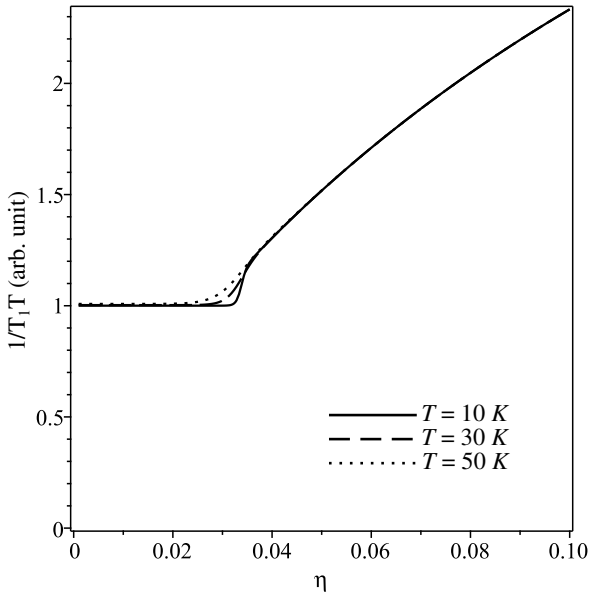

Figure 3.3.1: Spin-lattice relaxation rate as function of disorder, for: $T_F = 1000\ K$, $T_c = 10000\ K$, and for: $T = 10\ K$ (line), $T = 30\ K$ (dashed line), $T = 50\ K$ (dotted line)

limit), but this time we will consider a zero-gapped system.

The density of states was obtained by following the same steps as in the previous section. Here, the chemical potential will vary slightly in the interval of temperatures that goes from $T = 0$ K, up to room temperature ($\mu = E_F$ for $T = 0$ K and $\mu = 0.7E_F$ for $T = 300$ K), where E_F is the Fermi energy. Since we are interested in the effects of disorder on the spin-lattice relaxation time at low temperatures, we will approximate the chemical potential to $\mu \simeq E_F$.

In Fig. 3.3.1 we plot the spin-lattice relaxation rate as a function of disorder η, for three (low) temperatures. As long as disorder is very small, the spin-lattice relaxation rate reproduces the Fermi-gas behaviour. This result is in agreement with previous studies [19, 58]. However, in our model, even in the weak disorder limit, there is a critical value of the disorderness η_c that represents the threshold between the Fermi-gas (metallic) behaviour and a strong non-Fermi behaviour. The critical value is around $\eta_c \simeq 0.03$ for the parameters we used, and it is slightly dependent on temperature.

Our findings show that a very small amount of disorder leads to a Fermi-gas like behaviour of the studied relaxation rate. This behaviour changes drastically once the dimensionless concentration of impurities increases over a critical value η_c. If one would engineer an experiment

where the presence of disorder in the graphene system is carefully designed, then one could determine if the unitary limit is acceptable to describe the physical properties of graphene systems. Alongside the study we did on the static spin susceptibility [18], the results we obtained in this study could the used as an alternative test for the importance of the unitary limit in graphene systems and, thus, complement the previous studies on the conductivity [7], thermal and electric response [59].

3.4 Electronic heat capacity in disordered graphene systems

The constant interest for new materials that can be used in technological applications implies a need for the experimental and theoretical studies of such materials. This includes the thermal properties, as they can be of primary importance in certain applications. Graphene is such a materials and it is of interest to study its thermal properties (e.g., heat capacity and thermal conductivity) [22,23]. Close to the Dirac points, the energy dispersion of a graphene monolayer has a linear k dependence that at low temperature leads to an electronic heat capacity that is quadratic in temperature [60]. The dominant contribution to the heat capacity in graphene comes from the phonons, but the contribution from the electrons could be important. In the following we will summarise our findings on the electronic heat capacity of graphene systems in the presence of disorder.

The density of states used to determine the electronic heat capacity was the one determined in the previous section. In Fig. 3.4.1 we plot the scaled electronic heat capacity $C(T,\eta)/C_0$ (with $C_0 = k_B^3 T_c^2/(\pi v_F^2)$, where k_B is the Boltzmann constant, v_F is the Fermi speed, and $T_c = E_c/k_B$ with E_c being the energy cutoff) as a function of temperature for impurities concentration $\eta = 0.003$ and for the clean case. For the clean case we obtain $C(T,\eta=0) \sim T^2$, an expected result that is in agreement with Refs. [60–62] for the non-interacting case. On the other hand, in the presence of disorder and at low temperatures, the behaviour of the electronic heat capacity changes to $C(T,\eta) \sim T$. In order to obtain the analytical forms for these results, we introduced the varying parameter $x = (T_c/T)\sqrt{\eta/\ln(1/\eta)}$. The first case we considered was when $x \ll 1$. This case allowed us to take in the final result the limit $\eta \to 0$, which corresponds to the clean

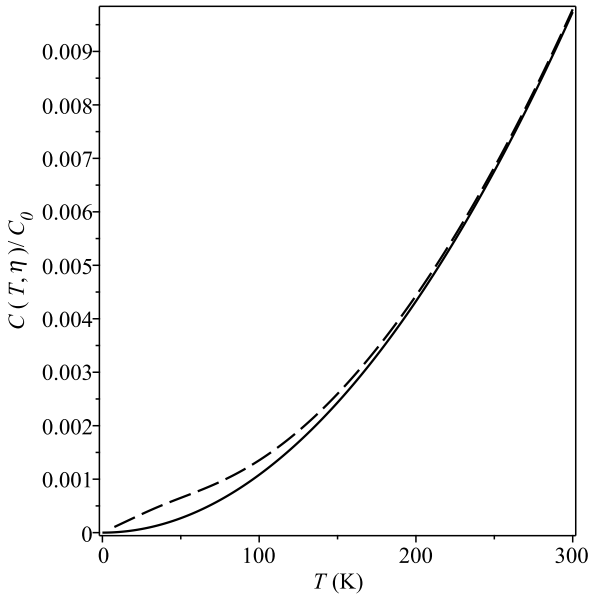

Figure 3.4.1: The scaled electronic heat capacity as a function of temperature is plotted with line for the clean case ($\eta = 0$) and dash-line in the presence of disorder ($\eta = 0.003$), for $T_c = 10000$ K

case. For very small values of η, we obtained:

$$C(T,\eta) \simeq \frac{9\zeta(3)k_B^3T^2}{\pi v_F^2}\left[1 - \frac{1}{54\pi\zeta(3)}\left(\frac{T_c}{T}\right)^4 \frac{\eta^2}{\ln\eta}\left(1 + \frac{3\pi}{4\ln\eta}\right)\right] \tag{3.4.1}$$

which reduces to:

$$C(T,\eta=0) = 9\zeta(3)C_0\left(\frac{T}{T_c}\right)^2 \tag{3.4.2}$$

when $\eta = 0$, in agreement with Ref. [60]. However, due to the fact that $f(\eta) = (\eta^2/\ln\eta)(1 + 3\pi/(4\ln\eta)) < 1$ for small η, the presence of disorder will enhance the electronic heat capacity, even for very small disorder. This enhancement is very small and appears due to the fact that a few electron states can nucleate on the impurities, thus enhancing the density of states. We should mention that $f(\eta) < 1$ for values of η between 0 and $e^{-3\pi/4} \simeq 0.095$. For this upper limit, if we take $T_c \sim 10000\ K$ and $T \sim 300\ K$ (room temperature), the parameter $x \simeq 6.7$. One concludes that Eq. (3.4.1) remains valid for degrees of disorder much lower than $\eta = 0.095$, to remain in agreement with the consideration $x \ll 1$. In the opposite case, we consider $x \gg 1$. This case corresponds to the presence of disorder (with η finite and positive) and $T_c/T \gg 1$

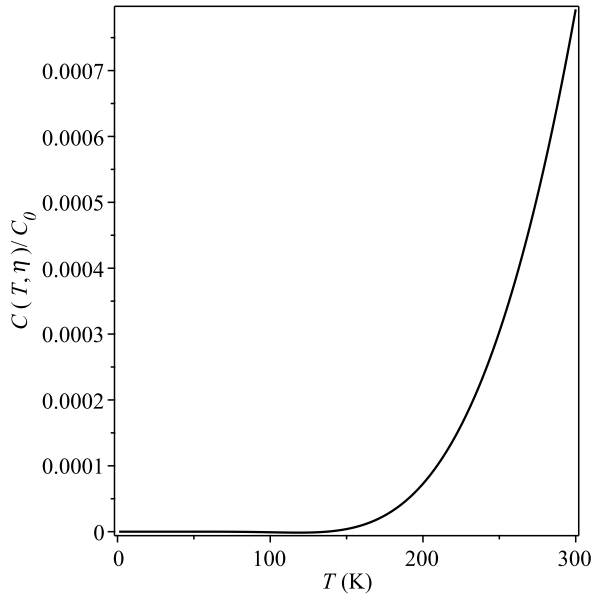

Figure 3.4.2: The scaled electronic heat capacity as a function of temperature is plotted for the extrinsic disordered graphene using the parameters: $Tc = 10000$ K, $T_F = 1000$ K, and $\eta = 0.003$

(low temperatures). The electronic heat capacity will be:

$$C(T,\eta) \simeq \frac{\pi}{3}\, C_0 \sqrt{-\eta \ln \eta}\, \frac{T}{T_c} \tag{3.4.3}$$

in agreement with the plot from Fig. 3.4.1. The electron states that at low temperatures nucleate on impurities enhance the electronic heat capacity. As the temperature increases, many of these states are washed out by the rising of temperature and the disordered electronic heat capacity becomes comparable to the clean case.

Now we will consider the extrinsic graphene case, when $\mu \neq 0$, and the Fermi temperature $T_F \sim 1000\ K$. In this case, the electron heat capacity has a temperature dependent chemical potential. However, for the values we used here: $T_c \sim 10000\ K$, $T_F \sim 1000\ K$, and $\eta \sim 0.003$; the chemical potential at room temperature is evaluated to $\mu(T = 300\ K) \simeq 0.85 \cdot E_F$ and we will assume the chemical potential to be $\mu \approx E_F$ in the $0 - 300\ K$ temperature range. In Fig. 3.4.2 we plot the scaled electronic heat capacity as a function of temperature for the case of extrinsic graphene. In this case, the electronic heat capacity is negligible small in a large low temperatures interval.

Thus, by using the parameter x, we found that the behaviour of the electronic heat capacity

could be quadratic (with a very small correction) in temperature through Eq (3.4.1) or linear through Eq (3.4.3). We have seen that small amounts of impurities could increase the value of the electronic heat capacity, while, on the other hand, for the extrinsic graphene case the electronic heat capacity could be negligibly small in a larger low temperatures interval. We found for low temperatures a somewhat similar result in Ref. [63], where they studied a monolayer hydrogenated graphene in the presence of impurities. In Ref. [64], by using the Random Phase Approximation, they found that in doped graphene the electronic heat capacity depends linearly on temperature. A finding similar to ours, for the case a non-interacting system with impurities and in the unitary limit.

This concludes our studies on disordered graphene systems with strong impurity scattering. The support for the use of the unitary limit is given in Ref. [7], where they found that the concentration dependence of the conductivity would indicate the dominant scatterers to be strong. Along other theoretical studies (e.g., Ref. [59]) we have proposed three more ways to test if the dominant scatters are in the unitary limit by studying the static spin susceptibility [18], the spin-lattice relaxation time [21], and the electronic heat capacity [24].

Chapter 4

Transition metal dichalcogenide superconductors

4.1 Introduction

Transition metal dichalcogenides are a class of quasi two-dimensional layers, bonded by weak van der Waals forces, that have a rich history spanning back over 50 years [25]. The synthesis of the first graphene monolayer [1] meant that free standing two-dimensional materials were possible and on top of that, it was found to be an exceptional material with many remarkable properties (e.g., the charge carriers are massless Dirac fermions). This discovery rejuvenated the research that was being done into transition metal dichalcogenides as well. The interest in this class of materials stems from their properties that have theoretical and experimental implications (such as applications in nano-electronics [65]). At low temperatures, these materials exhibit *s*-wave superconductivity and the superconductivity states coexist with charge density waves [26]. Other studies have revealed similar properties to those of high-temperature superconductors, such as the lifetime behaviour of the quasi-particles and the linear dependence of the normal state resistivity with temperature. On the other hand, in the region where the charge density waves gap vanishes, Dirac fermions quasi-particles are created. The superconductivity is then given by these particles that form acoustic phonon mediated Cooper-pairs [27,28]. They resemble to a degree the superconducting properties in graphene [29,30]. The superconductivity in transition metal dichalcogenides has been the subject of many studies [66–68]. In this chapter we will summarize our finding on transition metal dichalcogenides superconductors on a substrate.

In the presence of a substrate, an asymmetry occurs in the Hamiltonian. This is liable to lift

the degeneracy at the Dirac points and, as a consequence, a non-superconducting energy gap E_0 opens in the energy spectrum [20,31]. Close to the Dirac point this leads to the massive gapped spectrum and this is the case that we proposed to be studied, instead of the case of massless gapped spectrum [13] used in Ref. [32] to discuss the gap equation, the critical temperature, and the Geilikman-Kresin ratio [33, 34]. We will summarise the effect a substrate has on the superconducting energy gap at $T = 0$ K and close to the critical temperature. We will also present our studies on the specific heat, the specific heat jump, and the critical field.

4.2 General concepts

In 1911, H. Kamerlingh Onnes was the first to discover superconductivity [69]. The discovery of this entirely strange behaviour of some metals and alloys to have their electrical resistivity suddenly drop to zero and enter the superconducting state captivated the attention of the scientific community and it took them about four decades to formulate a satisfactory theoretical model. The zero electrical resistivity was demonstrated in experiments where they measured the electrical currents decay in solenoids. They concluded that it would take more than $100,000$ for the current to decay.

From other experiments, the scientists discovered that these materials were acting as perfect diamagnets [70]. They found that by cooling a superconductor down below its critical temperature, the magnetic field would be expulsed from the material and no other magnetic field would be able to enter. This phenomenon is called the Meissner effect and it suggested that perfect diamagnetism is a hallmark of the superconducting state. But this effect happens only for magnetic fields below a certain value, over which the superconducting state ceases to exist. The transition around this critical value of the field is reversible.

The first to describe the perfect conductivity and the Meissner effect were the London brothers in 1935 (the London equations) who proposed two equations to govern the microscopic and electric magnetic fields [71]. Using the London brothers' work, Pippard proposed an improved model [72]. They found that by using this model, one was able to fit the experimental data on tin and aluminium [73]. The London equations also lead to the definition of another fundamental characteristic to the superconductors, the London penetration depth λ_L. This length measures

the penetration depth of the external magnetic field.

In addition to the magnetic properties, the superconductors displayed distinct thermal properties. In zero field, the transition to the superconducting state is accompanied by a discontinuity in the specific heat, that in non-superconducting states varies linearly with the temperature. In superconductors, just below the critical temperature T_c, the electronic specific heat increases and then drops exponentially to zero as $T \to 0$ [74].

4.2.1 Superconductivity in transition metal dichalcogenides

Transition metal dichalcogenides have a long and rich history. The research that has already been done has proven their value from a theoretical perspective and applicability. The myriad of noteworthy properties, like the anomalous impurity effects in the superconducting phase [75]. Of notice is the fact that the anomalous properties of transition metal dichalcogenides do not depend on the sample as they tend to be very clean materials [28]. Still, the interpretation of the experimental data is very controversial due to fact that in the Peierls one-dimensional theory, the charge density wave gap if formed due to nested Fermi surfaces, while the nesting in two-dimensional systems is not perfect, which can lead to zero-gapped parts of the Fermi surface. There also seems to be a lack of consensus between the results obtained from different experimental investigation methods [28], scanning tunneling microscopy and angle resolved photoemission experiments, and the latter method even failing to detect traces of the charge density wave in the Brillouin zone.

Our following discussion will be based on Ref. [28], in which they proposed a model where the Fermi surface is fully gapped by the superposition of the charge density wave and s-wave superconducting order parameters. A charge density wave gap that is similar to the Brillouin zone of graphene (with the exception that the lattice inversion symmetry is broken) with nodes at the π-bands crossing points. This model has already been successfully used to explain several properties of two-dimensional transition metal dichalcogenides [76].

Usually, the Cooper pairs form across the Fermi sea surface, but in this case they form at the node points. The electron-phonon coupling is considered to piezoelectric in nature (a phenomenon that appears due to the broken inversion symmetry of the lattice). From the gap

equation, for $\mu = 0$, they found that it has a quantum critical point, which is a general property of the nodal liquids. When the parameter μ is modified, the superconducting gap Δ_S is strongly impacted and leads to the suppression of the quantum critical point. Two regimes were found for the scaling of Δ_S/μ: a weak coupling regime ("Fermi liquid") and a strong coupling regime (marginal limit). The specific heat jump from the BCS model is recovered for the Fermi liquid regime.

In the optical and thermal conductivities, they observed an infrared peak that stems from the quasi-particle excitations. This is a property that is not met in the more traditional superconductors. They also observed an anomalous suppression of the diamagnetic spectral-weight, which points to lack of high energy diamagnetic states in the superconducting gap.

4.3 Thermodynamic properties of transition metal dichalcogenide superconductors on a substrate

a) The superconducting gap

We analysed the superconducting gap Δ_s at zero and non-zero temperatures. At $T = 0\ K$, at the Dirac point ($\mu = 0$) we obtained the following result for the superconducting energy gap:

$$\Delta_s = v_F k_c \sqrt{\left(1 - \frac{g_c}{g}\right)^2 - \left(\frac{E_0}{v_F k_c}\right)^2} \tag{4.3.1}$$

where v_F is the Fermi velocity, k_c is a momentum cutoff, E_0 represents the energy gap induced by the substrate, g is the coupling constant, and with $g_c = 2\pi v_\Delta/k_c$ and the condition $g_c/g < 1$. In the absence of the substrate, when $E_0 = 0$, we re-obtain the result from [28]. However, notice that in our case the superconducting energy gap vanishes when $g_c/g = 1-(E_0/v_F k_c)$, otherwise, in the absence of the substrate it vanishes when $g_c/g = 1$. This means that the presence of the substrate reduces the value of the superconducting gap. Apart from the Dirac point ($\mu \neq 0$), the superconducting gap has a more complicated structure. Here, we will distinguished two cases:

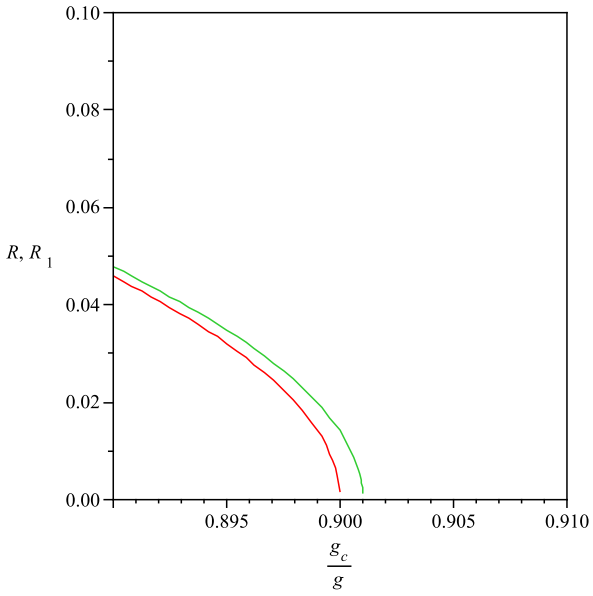

Figure 4.3.1: The ratio $R = \Delta_s/v_F k_c$ as a function of g_c/g for $\mu = 0$ (the lower curve - R_1) and $\mu/v_F k_c = 0.001$ (the upper curve - R). In both cases we used $E_0/v_F k_c = 0.01$

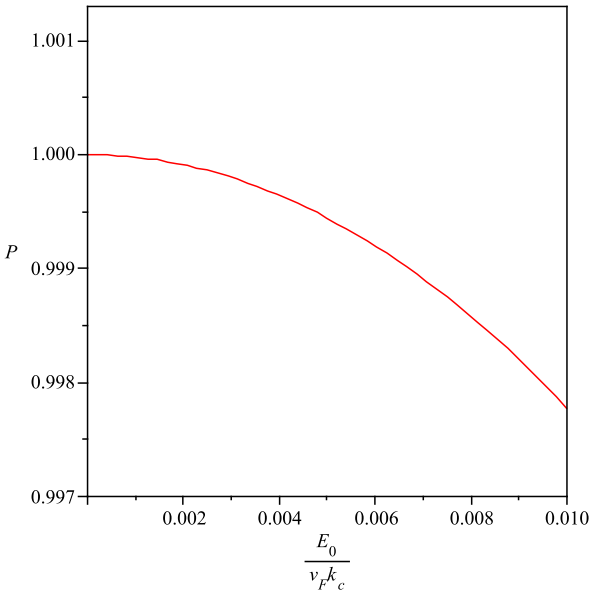

Figure 4.3.2: The ratio $P = \Delta_s(\mu, E_0)/\Delta_s(\mu, E_0 = 0)$ as a function of scaled energy $E_0/v_F k_c$, for $g_c/g = 0.85$ and $\mu/v_F k_c = 0.001$

I.) For $\mu \ll E_0$ and $\mu \ll \Delta_s$, the superconducting energy gap will be:

$$\Delta_s \simeq \frac{v_F k_c}{\sqrt{2}} \sqrt{\left(1 - \frac{g_c}{g}\right)^2 + \left(\frac{\mu}{v_F k_c}\right)^2} \sqrt{1 - \frac{2E_0^2}{a} + \sqrt{1 + \left(\frac{2\mu E_0}{a}\right)^2}} \tag{4.3.2}$$

where we used the notation $a = (v_F k_c)^2 (1 - g_c/g)^2 + \mu^2$. In Fig. 4.3.1 we plot the ratio $R = \Delta_s/v_F k_c$ as a function of g_c/g for $\mu = 0$ (lower curve) and for $\mu \neq 0$ (upper curve),

using the following parameters: $\mu/v_F k_c = 0.001$ and $E_0/v_F k_c = 0.01$. When $\mu \neq 0$ the superconducting gap is larger because this situation is more favourable for pairing.

In Fig. 4.3.2 we plot the ratio $P = \Delta_s(\mu, E_0)/\Delta_s(\mu, E_0 = 0)$ as a function of the scaled energy $E_0/v_F k_c$, using the following parameters $g_c/g = 0.85$, and $\mu/v_F k_c = 0.001$. We observe, again, that the presence of the substrate reduces the value of the superconducting gap even for the case when $\mu \neq 0$.

II.) For $\mu \gg E_0$ and $\mu \gg \Delta_s$, the superconducting gap will be:

$$\Delta_s \simeq 2\mu \exp\left[\frac{2\pi v_\Delta v_F}{\mu}\left(g_c^{-1} - g^{-1}\right) - 1 - \frac{E_0^2}{2\mu^2}\right] \tag{4.3.3}$$

Having found the superconducting gap at zero temperature, we turned to calculate the expressions for the superconducting gap at $T \neq 0\ K$. Here, we also discerned two cases. Considering $\mu > E_0$, $\beta_c(\mu - E_0)/2 \gg 1$, and $\beta_c(\mu + E_0)/2 \gg 1$ we found:

$$\Delta_s(T) \simeq \frac{\sqrt{1 - \frac{T}{T_c}}}{\sqrt{\frac{1}{2(\mu^2 - E_0^2)} + \frac{7\zeta(3)}{8(\pi k_B T_c)^2}}} \tag{4.3.4}$$

for $T < T_c$ and T close to T_c; where $\beta = 1/k_B T$ and k_B is the Boltzmann's constant (at $T = T_c$: $\beta = \beta_c$, where T_c is the critical temperature). Keeping the same temperature conditions, but in the opposite limit $\beta\mu \ll 1$, the superconducting gap will be (where $\Delta_0 = \sqrt{\alpha}\,(1 - g_c/g)$):

$$\Delta_s(T) \simeq 2\sqrt{\frac{T_c - T}{T_c}}\sqrt{\frac{\Delta_0}{\beta_c} + \frac{\mu^2 - E_0^2}{2}} \tag{4.3.5}$$

With $\beta_c\mu \ll 1$, we obtained the critical temperature:

$$T_c = \frac{\Delta_0 + \sqrt{\Delta_0^2 + (\mu^2 - E_0^2)\ln 4}}{\ln 16} \tag{4.3.6}$$

We notice that the substrate influences the superconducting energy gap, as well as the critical temperature, by reducing the effect of the chemical potential.

b) The specific heat

The specific heat jump is defined as the difference between the superconducting and the normal specific heat: $\Delta C = C_{V_S} - C_{V_N}$. We used Eq. (4.3.4) in order to evaluate $\Delta C|_{T=T_c}$ in the weak-coupling limit ($\beta_c\mu \gg 1$). Thus, we obtained:

$$\Delta C|_{T=T_c} \simeq \frac{k_B}{2\pi v_\Delta v_F \beta_c} \frac{\mu}{\frac{7\zeta(3)}{8\pi^2} + \frac{1}{2\beta_c^2\left(\mu^2 - E_0^2\right)}} \tag{4.3.7}$$

We also calculated the normal specific heat and the ratio $\Delta C/C_{V_N}|_{T=T_c}$ are:

$$C_{V_N}|_{\beta=\beta_c} \simeq \frac{\pi k_B \mu}{3 v_\Delta v_F \beta_c}\,, \qquad \left.\frac{\Delta C}{C_{V_N}}\right|_{T=T_c} \simeq \frac{3}{2\pi^2} \frac{1}{\frac{7\zeta(3)}{8\pi^2} + \frac{1}{2\beta_c^2\left(\mu^2 - E_0^2\right)}} \tag{4.3.8}$$

In the strong-coupling limit ($\beta_c\mu \ll 1$), using Eq. (4.3.5) we get:

$$\Delta C|_{T=T_c} \simeq \frac{8 k_B}{\pi v_\Delta v_F} \left(\frac{\ln 2}{\beta_c}\right)^2 \left[1 + \frac{\beta_c^2\left(\mu^2 - E_0^2\right)}{4\ln 2}\right] \tag{4.3.9}$$

In this case, the calculated normal specific heat and the ratio $\Delta C/C_{V_N}|_{T=T_c}$ are:

$$C_{V_N}|_{\beta=\beta_c} \simeq \frac{9\zeta(3) k_B}{\pi v_\Delta v_F \beta_c^2}\,, \qquad \left.\frac{\Delta C}{C_{V_N}}\right|_{T=T_c} \simeq \frac{8(\ln 2)^2}{9\zeta(3)} \left[1 + \frac{\beta_c^2\left(\mu^2 - E_0^2\right)}{4\ln 2}\right] \tag{4.3.10}$$

Having obtained these results, we observed that the presence of the substrate diminishes the effect of the chemical potential.

c) The critical field

The critical field for a superconducting material is the field above which the superconducting state cannot exist. This field is closely related to the critical temperature T_c and in zero field it is related to the free-energy difference between the superconducting and normal states. The transition is reversible and the superconducting state returns if the magnetic field drops below the critical field. For $\mu = 0$, we obtained for the critical field:, close to T_c:

$$H_c \simeq \sqrt{\frac{8}{v_\Delta v_F \beta_c}} \left(\Delta_0 - \frac{\beta_c E_0^2}{2}\right) \left(1 - \frac{T}{T_c}\right) \tag{4.3.11}$$

We find that the critical field has a linear dependence in temperature and that the presence of the substrate reduces the magnitude of the critical field. In the case $\mu \neq 0$, close to T_c the critical field obtained is:

$$H_c \simeq \sqrt{\frac{8}{v_\Delta v_F \beta_c}\left[1+\frac{1}{6}\left(\beta_c\mu\right)^2\right]}\left[\Delta_0+\frac{\beta_c}{2}\left(\mu^2-E_0^2\right)\right]\left(1-\frac{T}{T_c}\right) \tag{4.3.12}$$

In this case, we notice an increase of the factor in front of $(1 - T/T_c)$ compared to the one in Eq. (4.3.11), this translates in an increase of the critical field. This is an expected result due to the fact that a non-zero chemical potential is associated with an increased number of paired particles in the superconducting state.

d) Conclusions

We summarized the results we obtained for several thermodynamic properties of superconducting transition metal dichalcogenides on a substrate. The presence of the substrate lifts the degeneracy at the Dirac point and a non-superconducting energy gap E_0 occurs in the energy spectrum. The massless gapped spectrum has already been discussed in Ref. [32] and in this study we proposed to study the case of the massive gapped spectrum. The presence of the non-superconducting gap E_0 modifies the superconducting energy gap Δ_s. We've seen that in the presence of the substrate, the zero-temperature superconducting gap decreases, meaning that the pairing is less effective. In the case when the chemical potential is not at the Dirac point (i.e., $\mu \neq 0$), we notice an increase of the pairing energy due to an increase of the number of paired particles. At non-zero temperatures, and close to the critical temperature T_c, we noticed that the substrate influences the superconducting energy gap by reducing the influence of the chemical potential on the gap. The critical temperature is influenced in the same way. Once we had our results for the specific heat and specific heat jump at $T = T_c$, we noticed that, yet again, the substrate influences them by reducing the effect of the chemical potential.

When we analysed the critical field, we first considered the chemical potential at the Dirac point ($\mu = 0$) and found that the substrate reduces the magnitude of the critical field. A non-zero chemical potential has a positive effect on the critical field, but its effect is diminished

to some extent by the presence of the substrate. In both cases we noticed a linear temperature dependence of the critical field, but one should take notice that the critical temperature in Eq. (4.3.11) differs from the one in Eq. (4.3.12). Namely, in the first case the critical temperature is only influenced by the substrate (i.e., $T_c = T_c(E_0)$), while in the second case it is influenced by the substrate and the chemical potential (i.e., $T_c = T_c(E_0, \mu)$).

Chapter 5

Conclusions and Outlook

The field of two-dimensional materials is still growing and the need for better theoretical frameworks to understand the experimental data and to predict the properties of new materials will not cease to exist anytime soon. In this work we aimed to offer theoretical models of multiple properties of graphene and transition metal dichalcogenides.

Chapter 2 addresses the static spin susceptibility of graphene systems in the presence of disorder and an energy gap, with weak scatterers. We worked in the Born and the T-matrix approximation to determine the self-energy and the density of states of the system. By making use of the density of states we analysed the static spin susceptibility. We managed to achieve a qualitative agreement between our results and experimental data. Our model managed to capture of how certain aspects, concerning the influence the relative position of the chemical potential to the energy gap and the presence of weak scattering, influence the static spin susceptibility.

Chapter 3 addresses multiple properties of graphene systems in the presence of disorder with strong scatterers (the unitary limit). Thus, it is divided in multiple sections:

Section 3.2 studies the static spin susceptibility, for which we found that at zero temperature has a non-zero value and to have two different behaviours. Namely, if the impurities concentration is below a certain critical value, the static spin susceptibility has the same value at $T = 0$ K; over the critical value of disorder, the value of the zero temperature static spin susceptibility starts to increase.

Section 3.3 studies the spin-lattice relaxation. We found that the impurities concentration has a critical value that defines two different behaviours, as well. A very small amount of

disorder leads to a Fermi-gas like behaviour of the spin-lattice relaxation rate, over that critical value, this behaviour changes drastically.

Section 3.4 studies the heat capacity. We showed that, the heat capacity could have a quadratic or linear temperature dependence (depending on the value of a certain parameter x) and that a small amount of impurities could increase the value of the electronic heat capacity, while in the case of extrinsic graphene, its value could be negligible small in a larger low temperatures interval.

These results could be used to test if the scatterers in a graphene system are in the unitary limit and one would carefully engineer the presence of disorder in a graphene system, then, one could reveal if the unitary limit is indeed appropriate to describe the physical properties of graphene. We have to mention that the unitary limit has been successfully used to describe experimental data. We should mention, that the recent studies in Ref. [77] are in good agreement with the results we have achieved for the heat capacity.

Chapter 4 addresses the properties of a different two-dimensional system, transition metal dichalcogenides. While considering a massive gapped spectrum, we studied the influence a surface has on the superconducting energy gap, the specific heat and specific heat jump, and the critical field. The substrate decreases the superconducting gap and when we considered a non-zero chemical potential, the other properties were influenced by reducing the effect of the chemical potential.

A growing scientific field will always have room for improvement, be it by exploring new facets [78] or by improving already existing models. The results obtained in Chapter 2 could be altered if we would go beyond the methods used, by considering the self-consistent Born and T-matrix approximations. In Chapter 3, the model could be improved by considering the electron-electron effects on the density of states.

Bibliography

[1] A. K. Geim and K. S. Novoselov. The rise of graphene. *Nature Materials*, 6(3):183–191, 2007.

[2] P. R. Wallace. The band theory of graphite. *Physical Review*, 71(9):622–634, 1947.

[3] D P DiVincenzo and E J Mele. Self-consistent effective-mass theory for intralayer screening in graphite intercalation compounds. *Physical Review B*, 29(4):1685–1694, 1984.

[4] A. H. Castro Neto, F. Guinea, N. M R Peres, K. S. Novoselov, and A. K. Geim. The electronic properties of graphene. *Reviews of Modern Physics*, 81(1):109–162, 2009.

[5] S Das Sarma, Shaffique Adam, E H Hwang, and Enrico Rossi. Electronic transport in two-dimensional graphene. *Reviews of Modern Physics*, 83(2):407–470, 2011.

[6] N M R Peres, F Guinea, and A H Castro Neto. Electronic properties of disordered two-dimensional carbon. *Physical Review B*, 73(12):125411, 2006.

[7] P. M. Ostrovsky, I. V. Gornyi, and A. D. Mirlin. Electron transport in disordered graphene. *Physical Review B*, 74(23):235443, 2006.

[8] Mikito Koshino and Tsuneya Ando. Diamagnetism in disordered graphene. *Physical Review B*, 75(23):235333, 2007.

[9] Ben Yu-Kuang Hu, E. H. Hwang, and S. Das Sarma. Density of states of disordered graphene. *Physical Review B*, 78(16):165411, 2008.

[10] E H Hwang and S Das Sarma. Screening-induced temperature-dependent transport in two-dimensional graphene. *Physical Review B*, 79(16):165404, 2009.

[11] S. G. Sharapov and A. A. Varlamov. Anomalous growth of thermoelectric power in gapped graphene. *Physical Review B*, 86(3):035430, 2012.

[12] Aaron Bostwick, Taisuke Ohta, Jessica L. McChesney, Konstantin V. Emtsev, Thomas Seyller, Karsten Horn, and Eli Rotenberg. Symmetry breaking in few layer graphene films. *New Journal of Physics*, 9(10):385–385, 2007.

[13] L Benfatto and E Cappelluti. Spectroscopic signatures of massless gap opening in graphene. *Physical Review B*, 78(11):115434, 2008.

[14] T. L. Makarova, A. L. Shelankov, A. A. Zyrianova, A. I. Veinger, T. V. Tisnek, E. Lähderanta, A. I. Shames, A. V. Okotrub, L. G. Bulusheva, G. N. Chekhova, D. V. Pinakov, I. P. Asanov, and Ž. Šljivančanin. Edge state magnetism in zigzag-interfaced graphene via spin susceptibility measurements. *Scientific Reports*, 5(1):13382, 2015.

[15] I. Grosu and T.L. Biter. Spin susceptibility of disordered gapped graphene systems. *Physica E: Low-dimensional Systems and Nanostructures*, 86:154–157, 2017.

[16] K. S. Novoselov, A. K. Geim, S. V. Morozov, D. Jiang, M. I. Katsnelson, I. V. Grigorieva, S. V. Dubonos, and A. A. Firsov. Two-dimensional gas of massless Dirac fermions in graphene. *Nature*, 438(7065):197–200, 2005.

[17] Yuanbo Zhang, Yan-Wen Tan, Horst L. Stormer, and Philip Kim. Experimental observation of the quantum Hall effect and Berry's phase in graphene. *Nature*, 438(7065):201–204, 2005.

[18] I. Grosu and T.-L. Biter. Spin susceptibility as a test of unitary limit in disordered graphene systems. *Physica E: Low-dimensional Systems and Nanostructures*, 97:409–413, 2018.

[19] Balázs Dóra and Ferenc Simon. Unusual Hyperfine Interaction of Dirac Electrons and NMR Spectroscopy in Graphene. *Physical Review Letters*, 102(19):197602, 2009.

[20] Mircea Crisan, Ioan Grosu, and Ionel Ţifrea. NMR parameters in gapped graphene systems. *The European Physical Journal B*, 89(6):140, 2016.

[21] I. Grosu and T. L. Biter. Spin-lattice Relaxation Time in Disordered Graphene Systems. *Journal of Superconductivity and Novel Magnetism*, 31(6):1807–1811, 2018.

[22] Eric Pop, Vikas Varshney, and Ajit K. Roy. Thermal properties of graphene: Fundamentals and applications. *MRS Bulletin*, 37(12):1273–1281, 2012.

[23] F. Ma, H. B. Zheng, Y. J. Sun, D. Yang, K. W. Xu, and Paul K. Chu. Strain effect on lattice vibration, heat capacity, and thermal conductivity of graphene. *Applied Physics Letters*, 101(11):111904, 2012.

[24] I. Grosu and T. L. Biter. Electronic heat capacity in disordered graphene systems. *Physics Letters, Section A: General, Atomic and Solid State Physics*, 382(41):3042–3045, 2018.

[25] Stephen J. McDonnell and Robert M. Wallace. Atomically-thin layered films for device applications based upon 2D TMDC materials. *Thin Solid Films*, 616:482–501, 2016.

[26] R. L. Withers and J. A. Wilson. An examination of the formation and characteristics of charge-density waves in inorganic materials with special reference to the two- and one-dimensional transition- metal chalcogenides. *Journal of Physics C: Solid State Physics*, 19(25):4809–4845, 1986.

[27] A. H. Castro Neto. Charge density wave, superconductivity, and anomalous metallic behavior in 2D transition metal dichalcogenides. *Physical Review Letters*, 86(19):4382–4385, 2001.

[28] B. Uchoa, G. G. Cabrera, and A. H. Castro Neto. Nodal liquid and s -wave superconductivity in transition metal dichalcogenides. *Physical Review B - Condensed Matter and Materials Physics*, 71(18):184509, may 2005.

[29] N. B. Kopnin and E. B. Sonin. BCS Superconductivity of Dirac Electrons in Graphene Layers. *Physical Review Letters*, 100(24):246808, 2008.

[30] Teemu J. Peltonen, Risto Ojajärvi, and Tero T. Heikkilä. Mean-field theory for superconductivity in twisted bilayer graphene. *Physical Review B*, 98(22):220504, 2018.

[31] S. Y. Zhou, G. H. Gweon, A. V. Fedorov, P. N. First, W. A. De Heer, D. H. Lee, F. Guinea, A. H. Castro Neto, and A. Lanzara. Substrate-induced bandgap opening in epitaxial graphene. *Nature Materials*, 6(10):770–775, 2007.

[32] Ioan Grosu. Role of Substrate in Transition Metal Dichalcogenides Superconductivity. *Journal of Superconductivity and Novel Magnetism*, 33(10):3009–3013, 2020.

[33] B.T. Geilikman and V.Z. Kresin. About the connection between the transition temperature and the energy gap for superconductors with strong coupling. *Physics Letters A*, 40(2):123–124, 1972.

[34] B. Krunavakarn, P. Udomsamuthirun, S. Yoksan, I. Grosu, and M. Crisan. The gap-to-Tc ratio of a van Hove superconductor. *Journal of Superconductivity*, 11(2):271–273, 1998.

[35] K S Novoselov, A K Geim, S V Morozov, D Jiang, Y Zhang, S V Dubonos, I V Grigorieva, and A A Firsov. Electric Field Effect in Atomically Thin Carbon Films. *Science*, 306(5696):666–669, 2004.

[36] K. S. Novoselov, D. Jiang, F. Schedin, T. J. Booth, V. V. Khotkevich, S. V. Morozov, and A. K. Geim. Two-dimensional atomic crystals. *Proceedings of the National Academy of Sciences*, 102(30):10451–10453, 2005.

[37] R Peierls. Quelques propriétés typiques des corps solides. *Ann. Inst. Henri Poincaré*, 5:177–222, 1935.

[38] L. D. Landau. On the theory of phase transitions. *Zh. Eks. Teor. Fiz.*, 7(1937):19–32, 1937.

[39] Jw W McClure. Band Structure of Graphite and de Haas-van Alphen Effect. *Physical Review*, 108(3):612–618, 1957.

[40] J. C. Slonczewski and P. R. Weiss. Band Structure of Graphite. *Physical Review*, 109(2):272–279, 1958.

[41] P. R. Schroeder, M. S. Dresselhaus, and A. Javan. Location of Electron and Hole Carriers in Graphite from Laser Magnetoreflection Data. *Physical Review Letters*, 20(23):1292–1295, 1968.

[42] H Rydberg, M Dion, N Jacobson, E Schroder, P Hyldgaard, S I Simak, D C Langreth, and B I Lundqvist. Van der Waals density functional for layered structures. *Phys. Rev. Lett.*, 91(12):126402, 2003.

[43] Leonardo Spanu, Sandro Sorella, and Giulia Galli. Nature and Strength of Interlayer Binding in Graphite. *Physical Review Letters*, 103(19):196401, 2009.

[44] Xiaobin Chen, Fuyang Tian, Clas Persson, Wenhui Duan, and Nan-xian Chen. Interlayer interactions in graphites. *Scientific Reports*, 3(1):3046, 2013.

[45] E. Mostaani, N. D. Drummond, and V. I. Fal'ko. Quantum Monte Carlo Calculation of the Binding Energy of Bilayer Graphene. *Physical Review Letters*, 115(11):115501, 2015.

[46] Celso R C Rêgo, Luiz N Oliveira, Polina Tereshchuk, and Juarez L F Da Silva. Comparative study of van der Waals corrections to the bulk properties of graphite. *Journal of Physics: Condensed Matter*, 27(41):415502, 2015.

[47] Irina V. Lebedeva, Alexander V. Lebedev, Andrey M. Popov, and Andrey A. Knizhnik. Comparison of performance of van der Waals-corrected exchange-correlation functionals for interlayer interaction in graphene and hexagonal boron nitride. *Computational Materials Science*, 128:45–58, 2017.

[48] Ze Liu, Jefferson Zhe Liu, Yao Cheng, Zhihong Li, Li Wang, and Quanshui Zheng. Interlayer binding energy of graphite: A mesoscopic determination from deformation. *Physical Review B*, 85(20):205418, 2012.

[49] Wen Wang, Shuyang Dai, Xide Li, Jiarui Yang, David J Srolovitz, and Quanshui Zheng. Measurement of the cleavage energy of graphite. *Nature Communications*, 6(1):7853, 2015.

[50] M.I. Katsnelson and K.S. Novoselov. Graphene: New bridge between condensed matter physics and quantum electrodynamics. *Solid State Communications*, 143(1-2):3–13, 2007.

[51] Daniel R. Cooper, Benjamin D'Anjou, Nageswara Ghattamaneni, Benjamin Harack, Michael Hilke, Alexandre Horth, Norberto Majlis, Mathieu Massicotte, Leron Vands-

burger, Eric Whiteway, and Victor Yu. Experimental Review of Graphene. *ISRN Condensed Matter Physics*, 2012:1–56, 2012.

[52] Gerald D. Mahan. *Many-Particle Physics*. Springer US, Boston, MA, 2000.

[53] Tsuneya Ando. Screening Effect and Impurity Scattering in Monolayer Graphene. *Journal of the Physical Society of Japan*, 75(7):074716, 2006.

[54] Gerald Rickayzen. *Green's Functions and Condensed Matter*. Academic Press, 1980.

[55] Charles P. Slichter. *Principles of Magnetic Resonance*, volume 1 of *Springer Series in Solid-State Sciences*. Springer Berlin Heidelberg, Berlin, Heidelberg, 1990.

[56] A. Abragam. *The principles of nuclear magnetism*. Clarendon Press, Oxford, 1961.

[57] Hideaki Maebashi, Tomoki Hirosawa, Masao Ogata, and Hidetoshi Fukuyama. Nuclear Magnetic Relaxation and Knight Shift Due to Orbital Interaction in Dirac Electron Systems. *arXiv: 1709.02617*, pages 1–12, 2017.

[58] S. G. Sharapov, V. P. Gusynin, and H. Beck. Magnetic oscillations in planar systems with the Dirac-like spectrum of quasiparticle excitations. *Physical Review B*, 69(7):075104, 2004.

[59] Tomas Löfwander and Mikael Fogelström. Impurity scattering and Mott's formula in graphene. *Physical Review B*, 76(19):193401, 2007.

[60] Oskar Vafek. Anomalous Thermodynamics of Coulomb-Interacting Massless Dirac Fermions in Two Spatial Dimensions. *Physical Review Letters*, 98(21):216401, 2007.

[61] Wei Li and Guo Zhu Liu. Coulomb interaction and semimetal-insulator transition in graphene. *Physics Letters, Section A: General, Atomic and Solid State Physics*, 374(29):2957–2963, 2010.

[62] Pei Song He, Sung Jin Oh, Yu Chen, and Guang Shan Tian. Specific heat and magnetic susceptibility of graphene: A renormalization group study. *Communications in Theoretical Physics*, 54(5):897–907, 2010.

[63] Mohsen Yarmohammadi. Impurity doping effects on the orbital thermodynamic properties of hydrogenated graphene, graphane, in Harrison model. *Physics Letters, Section A: General, Atomic and Solid State Physics*, 380(48):4062–4069, 2016.

[64] M. R. Ramezanali, M. M. Vazifeh, Reza Asgari, Marco Polini, and A. H. MacDonald. Finite-temperature screening and the specific heat of doped graphene sheets. *Journal of Physics A: Mathematical and Theoretical*, 42(21):214015, 2009.

[65] Gianluca Fiori, Francesco Bonaccorso, Giuseppe Iannaccone, Tomás Palacios, Daniel Neumaier, Alan Seabaugh, Sanjay K. Banerjee, and Luigi Colombo. Electronics based on two-dimensional materials. *Nature Nanotechnology*, 9(10):768–779, 2014.

[66] Sudipta Koley, Narayan Mohanta, and Arghya Taraphder. Charge density wave and superconductivity in transition metal dichalcogenides. *The European Physical Journal B*, 93(5):77, 2020.

[67] Yu Zhang, Lin Li, Jin Hua Sun, Dong Hui Xu, Rong Lü, Hong Gang Luo, and Wei Qiang Chen. Kondo effect in monolayer transition metal dichalcogenide Ising superconductors. *Physical Review B*, 101(3):35124, 2020.

[68] Carmen Rubio-Verdú, Antonio M. García-García, Hyejin Ryu, Deung-Jang Choi, Javier Zaldívar, Shujie Tang, Bo Fan, Zhi-Xun Shen, Sung-Kwan Mo, José Ignacio Pascual, and Miguel M. Ugeda. Visualization of Multifractal Superconductivity in a Two-Dimensional Transition Metal Dichalcogenide in the Weak-Disorder Regime. *Nano Letters*, 20(7):5111–5118, 2020.

[69] M. Tinkham. *Introduction to Superconductivity*. McGraw-Hill, 1996.

[70] W. Meissner and R. Ochsenfeld. Ein neuer Effekt bei Eintritt der Supraleitfahigkeit. *Die Naturwissenschaften*, 21(44):787–788, 1933.

[71] H. London and F. London. The electromagnetic equations of the supraconductor. *Proceedings of the Royal Society of London. Series A - Mathematical and Physical Sciences*, 149(866):71–88, 1935.

[72] Alfred Brian Pippard and William Lawrence Bragg. An experimental and theoretical study of the relation between magnetic field and current in a superconductor. *Proceedings of the Royal Society of London. Series A. Mathematical and Physical Sciences*, 216(1127):547–568, 1953.

[73] A. B. Pippard. An experimental and theoretical study of the relation between magnetic field and current in a superconductor. *Proceedings of the Royal Society of London. Series A. Mathematical and Physical Sciences*, 216(1127):547–568, 1953.

[74] A.L. Fetter and J.D. Walecka. *Quantum Theory of Many-Particle Systems*. McGraw-Hill, 1971.

[75] D. A. Whitney, R. M. Fleming, and R. V. Coleman. Magnetotransport and superconductivity in dilute Fe alloys of NbSe2, TaSe2, and TaS2. *Physical Review B*, 15(7):3405–3423, 1977.

[76] A. H. Castro Neto. Charge Density Wave, Superconductivity, and Anomalous Metallic Behavior in 2D Transition Metal Dichalcogenides. *Physical Review Letters*, 86(19):4382–4385, 2001.

[77] Bobenko Nadezhda, Egorushkin Valery, and Melnikova Nataliya. Electron transport in disordered graphene and bigraphene. *Synthetic Metals*, 270(September):116590, 2020.

[78] V. N. Davydov. Role of the Lifshitz topological transitions in the thermodynamic properties of graphene. *RSC Advances*, 10(46):27387–27400, 2020.